Quantum Depletion of a Homogeneous Bose-Einstein Condensate

Raphael Lopes,[1,*] Christoph Eigen,[1] Nir Navon,[1,2] David Clément,[3] Robert P. Smith,[1] and Zoran Hadzibabic[1]
[1]Cavendish Laboratory, University of Cambridge, J.J. Thomson Avenue, Cambridge CB3 0HE, United Kingdom
[2]Department of Physics, Yale University, New Haven, Connecticut 06511, USA
[3]Laboratoire Charles Fabry, Institut d'Optique Graduate School, CNRS, Université Paris-Saclay, 91127 Palaiseau cedex, France
(Received 12 June 2017; published 7 November 2017)

We measure the quantum depletion of an interacting homogeneous Bose-Einstein condensate and confirm the 70-year-old theory of Bogoliubov. The observed condensate depletion is reversibly tunable by changing the strength of the interparticle interactions. Our atomic homogeneous condensate is produced in an optical-box trap, the interactions are tuned via a magnetic Feshbach resonance, and the condensed fraction is determined by momentum-selective two-photon Bragg scattering.

DOI: 10.1103/PhysRevLett.119.190404

After the superfluidity of liquid ^{4}He was discovered in 1937 [1,2], its connection to Bose-Einstein condensation was posited by London [3] and Tisza [4]. However, while at zero temperature liquid helium is 100% superfluid, less than 10% of the atoms are actually in the Bose-Einstein condensate (BEC) [5,6]; most of the particles are coherently expelled from the condensate by strong interactions and spread over a wide range of momenta. In 1947, Bogoliubov developed a theory that explains the microscopic origin of such interaction-driven, quantum depletion of a BEC [7]. This theory has become a cornerstone of our conceptual understanding of quantum fluids but is quantitatively valid only for relatively weak interactions and could not be tested with liquid helium. The connection between condensation and superfluidity, as well as superconductivity, is still a topic of active discussion; for a modern perspective, see [8,9].

Nowadays, gaseous atomic BECs provide a flexible setting for exploring the rich physics of interacting Bose fluids [10–12], and many liquid-helium-inspired theories can now be directly confronted with experiments. According to the Bogoliubov theory, for a homogeneous Bose gas of particle density n and interactions characterized by the scattering length a, and assuming $\sqrt{na^3} \ll 1$, the condensed fraction at zero temperature is [13]

$$n_{\mathrm{BEC}}/n = 1 - \gamma\sqrt{na^3}, \tag{1}$$

where $\gamma = 8/(3\sqrt{\pi}) \approx 1.5$. This prediction was tested using diffusion Monte Carlo simulations and found to be quantitatively valid for $na^3 \lesssim 10^{-3}$ [14], but an experimental confirmation has been lacking. Effects of quantum depletion have been observed in harmonically trapped atomic gases, both by enhancing the role of interactions in optical lattices [15] (see also [16,17]) and in high-resolution studies of the expansion of a weakly interacting gas [18]. However, only semiquantitative comparison with the theory has been possible, due to complications associated with the addition of the lattice, the inhomogeneity of the clouds, and/or the interpretation of the expansion measurements [19].

In this Letter, we test and verify the Bogoliubov theory of quantum depletion in a textbook setting, using a homogeneous ^{39}K BEC [20]. We produce our clouds in a cylindrical optical-box trap (see Fig. 1), of radius $R = 32\ \mu$m and length $L = 50\ \mu$m [21], tune the interaction strength via a magnetic Feshbach resonance [22], and measure the condensed fraction by spectroscopic "BEC filtering" [23]—using Doppler-sensitive two-photon Bragg scattering [24,25], we *spatially* separate the BEC from the high-momentum components of the gas.

Bragg spectroscopy of ultracold atomic gases [24,25] gives access to the dynamic structure factor $S(q,\omega)$ in conceptually the same way as inelastic neutron scattering does for liquid helium [5,6]; here $\hbar q$ and $\hbar\omega$ are the momentum and energy, respectively, of an excitation. We briefly highlight some differences between our measurements and those performed on liquid helium. First, after preparing a strongly interacting gas and just before probing it, we suddenly turn off the interactions. This eliminates final-state interaction effects and allows the clean and direct probing of the suddenly frozen momentum distribution. Second, in our experiments, the momentum $\hbar\mathbf{q}$ is imparted to an atom via a stimulated (coherent) two-photon process, and $\mathbf{q}$ and ω are defined by the differences in the momenta and frequencies of the photons from two intersecting laser beams. In an equivalent picture, the atom's energy changes through *elastic* scattering off a *moving* optical-lattice potential, formed by the interference of the two laser beams, which has period $2\pi/q$ and speed ω/q. For an atom with initial momentum $\hbar\mathbf{k}$, the scattering resonance is given by $\omega = \hbar q^2/(2m) + \hbar\mathbf{k}\cdot\mathbf{q}/m$, where m is the atom mass and the $\mathbf{k}\cdot\mathbf{q}$ term arises due to the Doppler effect. This $\mathbf{k}$ dependence of the scattering resonance allows a spectroscopic measurement of the momentum distribution

 © 2017 American Physical Society

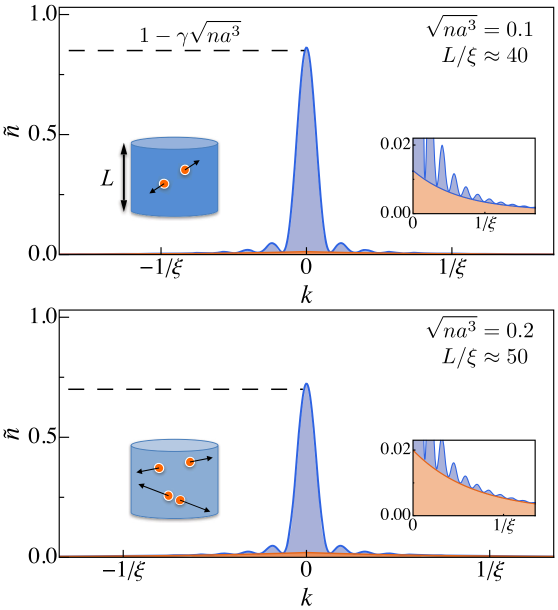

FIG. 1. Momentum distribution of a zero-temperature homogeneous Bose gas. We consider a gas of density n and size L and two different values of the scattering length a. We show the expected 1D momentum distribution $\tilde{n}(k)$ (see the text), normalized so that $\tilde{n}(0) = 1$ would correspond to no quantum depletion [setting γ in Eq. (1) to 0]. The total $\tilde{n}(k)$ consists of the BEC peak (blue), with a Heisenberg-limited width $\propto 1/L$, and a broad quantum-depletion pedestal (orange) of characteristic width $1/\xi$, where ξ is the healing length. To a good approximation, the low-k distribution is the same as for a pure BEC, just scaled by a factor of $1-\gamma\sqrt{na^3}$, indicated by the dashed lines. For this illustration, we use experimentally relevant values of L/ξ, but exaggerated values of $\sqrt{na^3}$, to make the orange shading visible in the main panels. Also note that we assume that the very broad $\tilde{n}_{\rm QD}(k)$ is not affected by finite-size effects. The cartoons on the left depict the coherent excitations out of the (blue) condensate, which occur as pairs of atoms with opposite momenta. The right insets highlight the fact that $\tilde{n}_{\rm QD}(k) \gg \tilde{n}_{\rm BEC}(k)$ at large k.

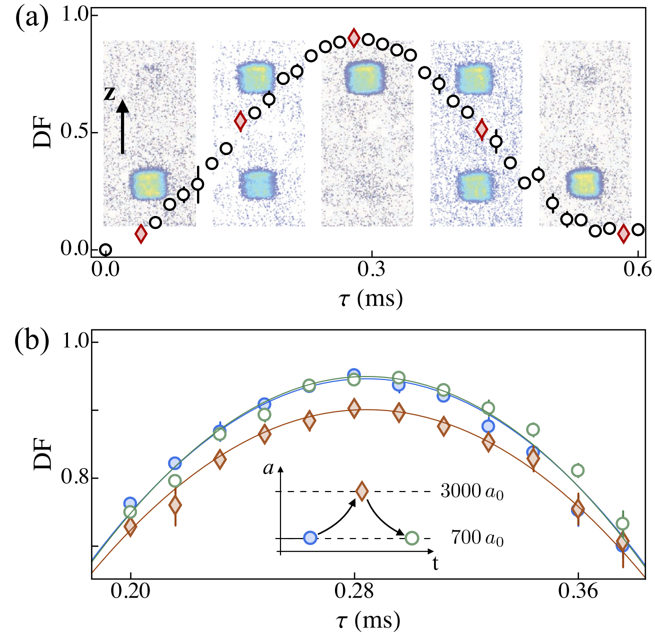

FIG. 2. Bragg filtering and reversible interaction tuning of the condensed fraction. (a) Diffracted fraction (DF) as a function of the Bragg pulse duration τ for $\Omega = 2\pi \times 1.8$ kHz and $a \approx 3000a_0$. Absorption images in the background show the stationary (bottom) and diffracted (top) clouds, for the data points indicated by the red diamonds. (b) Diffracted fraction for τ close to π/Ω, for three different preparations of the cloud (see the inset): at $700a_0$ (solid blue circles), after raising a from $700a_0$ to $3000a_0$ in 80 ms (orange diamonds), and after reducing it back to $700a_0$ in another 80 ms (open green circles). We see that increasing a reversibly reduces the maximal diffracted fraction. All error bars show standard statistical errors in the mean.

and, hence, the condensed fraction. Finally, note that, since the atomic states $|\mathbf{k}\rangle$ and $|\mathbf{k}+\mathbf{q}\rangle$ are coherently coupled by the Bragg beams, an atom undergoes Rabi oscillations between the two states as a function of the duration of the Bragg light pulse, with a period set by the two-photon Rabi frequency Ω [see Fig. 2(a)].

In our setup [26], $\mathbf{q}$ is aligned with the axis of the cylindrical box trap (z) and $q = 1.7 \times 2\pi/\lambda$, where $\lambda = 767$ nm. The Bragg resonance condition thus depends only on an atom's initial momentum along z, and by counting the diffracted atoms we effectively probe the one-dimensional (1D) momentum distribution of the cloud, $\tilde{n}(k)$, given by the integral of the 3D distribution along the two transverse directions. We aim to diffract only the condensed atoms, so we tune ω to $\hbar q^2/(2m)$. In frequency space, our spectroscopic resolution is set by Ω, which corresponds to a momentum resolution of $\Omega m/q$.

More specifically, we want to spatially separate the BEC from the quantum depletion (QD), which relies on a separation of three momentum scales, $1/L \ll 1/\xi \ll q$, where $\xi = 1/\sqrt{8\pi na}$ is the healing length. In Fig. 1, we illustrate the expected $\tilde{n}(k)$ for a zero-temperature gas: $\tilde{n}(k) = \tilde{n}_{\rm BEC}(k) + \tilde{n}_{\rm QD}(k)$, where $\tilde{n}_{\rm BEC}$ has a Heisenberg-limited width $\propto 1/L$ [27] and exponentially suppressed high-k tails, while $\tilde{n}_{\rm QD}(k)$ has a width $\propto 1/\xi$ and long polynomial tails [18,28–30] (see [31] for details). The inequality $L/\xi \gg 1$ thus ensures that $\tilde{n}_{\rm QD}(k)$ extends over a much wider range of momenta than $\tilde{n}_{\rm BEC}(k)$, so Ω can be chosen such that a Bragg pulse diffracts essentially the whole BEC and almost none of the QD. The inequality $q\xi \gg 1$ ensures that the momentum kick received by a diffracted atom, $\hbar q$, is much larger than the QD momentum spread, so that, after the Bragg pulse and a sufficiently long subsequent time-of-flight, the diffracted and the nondiffracted portions of the cloud clearly separate in real space [see Fig. 2(a)]. For all our measurements, $L/\xi > 30$ and $q\xi > 12$.

We start by producing a quasipure weakly interacting BEC of density $n \approx 3.5 \times 10^{11}$ cm^{-3} in the lowest ^{39}K hyperfine state, $|F = 1, m_F = 1\rangle$ in the low-field basis, which features a Feshbach resonance centred at 402.70(3) G [32]. We prepare the BEC at $a = 200a_0$, where a_0 is the Bohr radius, so $\sqrt{na^3} < 10^{-3}$, and in the time-of-flight expansion we do not discern any thermal fraction. We then (in 150–250 ms) increase a to a value in the range 700–3000a_0 and measure the condensed fraction. To prepare the initial quasipure BEC, we lower the trap depth U_0 to $\approx k_B \times 20$ nK, but before increasing a we adiabatically raise U_0 by a factor of 5, to ensure that $U_0 \gg \hbar^2/(2m\xi^2)$. The largest a that we explore here is limited by imposing requirements that (i) during the whole experiment the atom loss due to three-body recombination is $< 10\%$, and (ii) if we reduce a back to $200a_0$, we do not observe any signs of heating; for a discussion of additional measurements at even larger a (with larger particle loss), see [31].

Just before turning off the trap and applying the Bragg pulse, we rapidly (in 60 μs) turn off the interactions, using a radio-frequency pulse to transfer the atoms to the $|F = 1, m_F = 0\rangle$ state, in which $a \approx 0$ [32]. This freezes the momentum distribution before we probe it and allows the diffracted and nondiffracted components of the gas to separate in space without collisions.

After the Bragg pulse, we wait for 10 ms and then take an absorption image along a direction perpendicular to z [see Fig. 2(a)]. In 10 ms, the diffracted and nondiffracted portions of the gas separate by $\approx$220 μm, while neither expands significantly beyond the original size of the box-trapped cloud.

In Fig. 2(a), we show a typical variation of the diffracted fraction of the gas with the duration of the Bragg pulse, τ, for our chosen $\Omega = 2\pi \times 1.8$ kHz (see [31]). In the background, we show representative absorption images of the stationary (bottom) and diffracted (top) clouds.

Assuming that we perfectly filter out the condensate from the high-k components of the gas, the condensed fraction of the cloud is given by the maximal diffracted fraction, η, observed for $\tau = \pi/\Omega \approx 0.28$ ms. We see that η is slightly below unity, which is expected due to quantum depletion but can in practice also be observed for other reasons, including experimental imperfections and the inevitably nonzero temperature of the cloud. It is therefore important that our measurements are differential—we study the variation of η with a while keeping other experimental parameters the same. It is also crucial to verify that the tuning of η with a is adiabatically reversible, which excludes the possibility that the condensed fraction is reduced due to nonadiabatic heating or losses.

In Fig. 2(b), we focus on $\tau \approx \pi/\Omega$ and show measurements for three different experimental protocols: for a cloud prepared at $700a_0$, after increasing a to $3000a_0$, and after reducing it back to $700a_0$ (see the inset). We see that η is indeed reduced when a is increased and also that this effect is fully reversible (within experimental errors); we have verified such reversibility for our whole experimental range of a values.

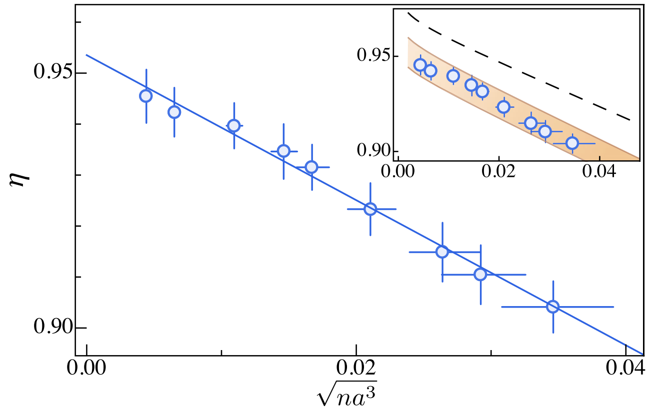

FIG. 3. Measurement of the quantum depletion. We plot the maximal diffracted fraction η versus the interaction parameter $\sqrt{na^3}$. A linear fit (solid line) gives $\eta(0) = 0.954(5)$ and $\gamma = 1.5(2)$. Vertical error bars show fitting errors, while horizontal ones reflect the uncertainty in the position of the Feshbach resonance and a 10% uncertainty in n. Inset: Analysis of systematic effects. We show numerical simulations for $T = 0$ (dashed line) and for initial temperatures (at $a = 200a_0$) between 3.5 and 5 nK (orange shading, from top to bottom); see the text and [31] for more details.

In Fig. 3, we summarize our measurements of the variation of η with the interaction parameter $\sqrt{na^3}$. We observe the expected linear dependence, with $\eta(0)$ close to unity. Fitting the data with $\eta(0)(1 - \gamma\sqrt{na^3})$ gives $\gamma = 1.5(2)$, in agreement with Eq. (1).

Finally, we numerically assess the systematic effects on γ due to noninfinite L/ξ and a small nonzero temperature T, which are both $\lesssim$20% and partially cancel. The results of this analysis are shown in the inset in Fig. 3; for details, see [31]. The dashed line shows the simulated η for $T = 0$ and our values of n, L, and Ω. For any noninfinite Ω, the tails of the BEC momentum distribution are not fully captured by the Bragg pulse, which slightly reduces $\eta(0)$. More importantly, we diffract some of the quantum-depletion atoms, which reduces the apparent γ. A linear fit (omitted for clarity) gives that for $T = 0$ we actually expect $\gamma \approx 1.2$. The small systematic differences between our data and this simulation can be explained by a small nonzero temperature. A nonzero temperature generally reduces η due to thermal depletion, the momentum tails of which are not diffracted by the Bragg pulse. Moreover, if the gas is initially prepared (at $200a_0$) at a small $T > 0$, this does not merely reduce η by a constant offset (independent of $\sqrt{na^3}$) but slightly increases the apparent γ; even adiabatically increasing a increases the thermal depletion, because it modifies both the dispersion relation and the particle content of the thermally populated low-k excitations [28,31]. As indicated by the orange shaded region, our data are consistent with an initial T between 3.5 and 5 nK; this is compatible with the fact that we do not discern the corresponding thermal fractions of $\lesssim 10\%$ in time-of-flight expansion at $200a_0$, and is reasonable for our trap depth of ≈ 20 nK. Due to these effects, the expected dependence of η on $\sqrt{na^3}$ is also not perfectly linear, but this effect is negligible on the scale of the experimental errors.

In conclusion, within a 15% statistical error and 20% systematic effects, we have quantitatively confirmed the Bogoliubov theory of quantum depletion of a Bose-Einstein condensate, which is one of the cornerstones of our understanding of interacting quantum fluids. The largest interaction strength that we could reliably explore is already at the limit of agreement between Bogoliubov's analytical theory and Monte Carlo simulations; adiabatically increasing $\sqrt{na^3}$ by another factor of 2 should allow quantitative studies of the regime where the two theories disagree at the level of our demonstrated experimental precision (see [31]). The methods employed here could be extended to study the momentum distribution of the quantum depletion and could also be useful for sensitive thermometry of homogeneous ultracold Bose gases.

Data supporting this publication are available for download at [33].

We thank Richard Fletcher and Fabrice Gerbier for inspiring discussions. This work was supported by the Royal Society, EPSRC [Grant No. EP/N011759/1], ERC (QBox), AFOSR, and ARO. R. L. acknowledges support from the EU Marie-Curie program [Grant No. MSCA-IF-2015 704832] and Churchill College, Cambridge. N. N. acknowledges support from Trinity College, Cambridge. D. C. acknowledges support from the Institut Universitaire de France.

*rl531@cam.ac.uk

[1] P. Kapitza, Nature (London) **141**, 74 (1938).
[2] J. F. Allen and A. D. Misener, Nature (London) **141**, 75 (1938).
[3] F. London, Phys. Rev. **54**, 947 (1938).
[4] L. Tisza, Phys. Rev. **72**, 838 (1947).
[5] A. Miller, D. Pines, and P. Nozières, Phys. Rev. **127**, 1452 (1962).
[6] H. R. Glyde, S. O. Diallo, R. T. Azuah, O. Kirichek, and J. W. Taylor, Phys. Rev. B **84**, 184506 (2011).
[7] N. N. Bogoliubov, J. Phys. (USSR) **11**, 23 (1947).
[8] A. J. Leggett, *Quantum Liquids* (Oxford University Press, New York, 2006).
[9] *BCS-BEC Crossover and the Unitary Fermi Gas*, edited by W. Zwerger (Springer, New York, 2011).
[10] F. Dalfovo, S. Giorgini, L. P. Pitaevkii, and S. Stringari, Rev. Mod. Phys. **71**, 463 (1999).
[11] I. Bloch, J. Dalibard, and W. Zwerger, Rev. Mod. Phys. **80**, 885 (2008).
[12] F. Chevy and C. Salomon, J. Phys. B **49**, 192001 (2016).
[13] T. D. Lee, K. Huang, and C. N. Yang, Phys. Rev. **106**, 1135 (1957).
[14] S. Giorgini, J. Boronat, and J. Casulleras, Phys. Rev. A **60**, 5129 (1999).
[15] K. Xu, Y. Liu, D. E. Miller, J. K. Chin, W. Setiawan, and W. Ketterle, Phys. Rev. Lett. **96**, 180405 (2006).
[16] M. Greiner, M. O. Mandel, T. Esslinger, T. Hänsch, and I. Bloch, Nature (London) **415**, 39 (2002).
[17] M. Köhl, T. Stöferle, H. Moritz, C. Schori, and T. Esslinger, Appl. Phys. B **79**, 1009 (2004).
[18] R. Chang, Q. Bouton, H. Cayla, C. Qu, A. Aspect, C. I. Westbrook, and D. Clément, Phys. Rev. Lett. **117**, 235303 (2016).
[19] C. Qu, L. P. Pitaevskii, and S. Stringari, Phys. Rev. A **94**, 063635 (2016).
[20] C. Eigen, A. L. Gaunt, A. Suleymanzade, N. Navon, Z. Hadzibabic, and R. P. Smith, Phys. Rev. X **6**, 041058 (2016).
[21] A. L. Gaunt, T. F. Schmidutz, I. Gotlibovych, R. P. Smith, and Z. Hadzibabic, Phys. Rev. Lett. **110**, 200406 (2013).
[22] C. Chin, R. Grimm, P. Julienne, and E. Tiesinga, Rev. Mod. Phys. **82**, 1225 (2010).
[23] F. Gerbier, J. H. Thywissen, S. Richard, M. Hugbart, P. Bouyer, and A. Aspect, Phys. Rev. A **70**, 013607 (2004).
[24] M. Kozuma, L. Deng, E. W. Hagley, J. Wen, R. Lutwak, K. Helmerson, S. L. Rolston, and W. D. Phillips, Phys. Rev. Lett. **82**, 871 (1999).
[25] J. Stenger, S. Inouye, A. P. Chikkatur, D. M. Stamper-Kurn, D. E. Pritchard, and W. Ketterle, Phys. Rev. Lett. **82**, 4569 (1999).
[26] R. Lopes, C. Eigen, A. Barker, K. G. H. Viebahn, M. Robert-de-Saint-Vincent, N. Navon, Z. Hadzibabic, and R. P. Smith, Phys. Rev. Lett. **118**, 210401 (2017).
[27] I. Gotlibovych, T. F. Schmidutz, A. L. Gaunt, N. Navon, R. P. Smith, and Z. Hadzibabic, Phys. Rev. A **89**, 061604 (2014).
[28] C. J. Pethick and H. Smith, *Bose-Einstein Condensation in Dilute Gases* (Cambridge University Press, Cambridge, England, 2002).
[29] R. J. Wild, P. Makotyn, J. M. Pino, E. A. Cornell, and D. S. Jin, Phys. Rev. Lett. **108**, 145305 (2012).
[30] P. Makotyn, C. E. Klauss, D. L. Goldberger, E. A. Cornell, and D. S. Jin, Nat. Phys. **10**, 116 (2014).
[31] See Supplemental Material at http://link.aps.org/supplemental/10.1103/PhysRevLett.119.190404 for details on the momentum distributions, numerical simulations of the finite-size and nonzero-temperature effects, and tentative measurements at even higher interaction strengths, which hint at a deviation from the Bogoliubov theory.
[32] R. J. Fletcher, R. Lopes, J. Man, N. Navon, R. P. Smith, M. W. Zwierlein, and Z. Hadzibabic, Science **355**, 377 (2017).
[33] https://doi.org/10.17863/CAM.13808.